

Bounds on neutrino magnetic moment tensor from solar neutrinos

Anjan S. Joshipura and Subhendra Mohanty
 Physical Research Laboratory, Navrangpura, Ahmedabad - 380 009, India

Solar neutrinos with non-zero magnetic moments will contribute to the electron scattering rates in the Super-Kamokande experiment. The magnetic moment scattering events in Super-K can be accommodated in the standard VO or MSW solutions by a change of the parameter space of mass square difference and mixing angle but the shifted neutrino parameters obtained from Super-K will (for some values of neutrino magnetic moments) become incompatible with the fits from SNO, Gallium and Chlorine experiments. We compute the upper bounds on the Dirac and Majorana magnetic moments of solar neutrinos by simultaneously fitting all the observed solar neutrino rates. The bounds the magnetic moment matrix elements are of the order of 10^{-10} B.

1. Introduction

Solar neutrino experiments with Chlorine [1], Gallium [2], and water Cerenkov detectors [3], [4], show that there is a deficit of e^- at the Earth compared to the predictions [5] of the standard solar model (SSM). It is commonly accepted that vacuum oscillations (VO) or matter induced MSW conversions, with large mixing angle (LMA) or small mixing angle (SMA), can account for the deficit of solar neutrinos. The available experimental results allow not only a test of the neutrino oscillation hypothesis but also offer possibilities of constraining new physics, e.g. neutrino magnetic moment [6-8], neutrino decay [9], flavor changing neutral currents, etc.

Neutrinos with non-zero magnetic moments will contribute to the e^- scattering rates at Super-K. The electron scattering rate at Super-K (defined as the ratio of average number of electron scatterings observed and the theoretical prediction of e^-e^- elastic scattering in SSM) is given by

$$R_{SK} = \frac{1}{h_{e^-i}} (h_{e^-e^-i} + h_{(1 - P_{ee})i} + h_{magi}) \quad (1)$$

Here the first two terms denote the standard e^-e^- and e^- scattering processes respectively, P_{ee} being the e^- survival probability. The last term in eq.(1) corresponds to the scattering events $e^- \rightarrow e^-$ due to non-zero neutrino magnetic moments. Unlike Super-K and SNO, the other solar detectors do not probe the neutral current interactions and are thus not sensitive to the magnetic moment scattering. The previous bounds on neutrino magnetic moment from solar neutrinos have made use of the only Super-K results [6,7] or have combined Super-K and SNO results [8] together. The other experiments however indirectly influence the bound on magnetic moment through a combined chi-square analysis. We use results from all experiments here concentrating mainly on rates to put bounds on elements of the magnetic moment tensor $_{ij}$ defined in the neutrino mass basis.

The magnetic moment scatterings are helicity flipping processes and are more appropriately described in the mass basis unlike the non- $\bar{p}p$ weak interaction processes which are described in the flavor basis. The electron neutrinos produced at the Sun arrive as a linear combination of mass eigenstates at the detector. The probability amplitude of the i mass eigenstate at the detector is denoted by $A_{il}(L)$ and $e^- \rightarrow e^-$ scattering amplitude is proportional to $_{ij}$. It is assumed [7] that prior to scattering the neutrinos are a linear combination of different mass eigenstates, but after scattering the neutrino beam is an incoherent sum of different mass states. The probability amplitude of the i mass eigenstate at the detector is denoted by $A_{il}(L)$ and the $e^- \rightarrow e^-$ scattering amplitude is proportional to $_{ij}$. The magnetic moment differential scattering cross section at the detector is then given by

$$\frac{d_{mag}}{dT} = \frac{2}{eff} \frac{1}{m_e^2} \left(\frac{1}{T} - \frac{1}{E} \right) \quad (2)$$

T is the recoil energy of the electrons, E the initial neutrino energy and the magnetic moments $_{ij}$ are in units of Bohr magneton. The effective magnetic moment $_{eff}$ can be written in terms of the intrinsic neutrino magnetic moments $_{ij}$ as

$$_{eff}^2 = \sum_j \sum_i A_{il} \frac{X}{m_i} \frac{X}{m_j} \frac{_{ij}^2}{_{il}^2} \quad (3)$$

The magnetic moment tensor $_{ij}$ is antisymmetric if neutrinos are Majorana particles. For Dirac neutrinos, $_{ij}$ are arbitrary complex numbers but in special case of CP conserving theory, they are real and symmetric [6]. We shall assume this to be the case. The amplitude A_{il} of the i mass eigenstate at the detector depends upon the oscillation model which solves the solar neutrino problem.

We consider the case of vacuum oscillations, and matter induced MSW conversions in turn and derive bounds on $_{ij}$ for each of these cases separately.

2. Vacuum Oscillations

Neutrinos are produced in the solar core as the e flavor eigenstate, and the amplitude for detecting them at a distance L as a mass eigenstate is given by

$$A_i(L) = U_{ei} e^{iE_i L} : \quad (4)$$

The elements of mixing matrix U are constrained by atmospheric neutrino and CHOOZ experiments to be of the following form :

$$\begin{matrix} 0 & 1 & 0 \\ e & & \\ @ & A = @ & \\ & c_1 & s_1 & 1 & 0 & 1 \\ & c_2 s_1 & c_2 c_1 & s_2 & A & @ \\ & s_2 s_1 & s_2 c_1 & c_2 & & 3 \end{matrix} : \quad (5)$$

We have approximated $U_{e3} = 0$ in order to account for the negative results obtained in e disappearance experiment at CHOOZ [10]. The small value of U_{e3} (taken here as zero) also prevents the mixing of the third neutrino in vacuum. In addition to the above mixing one also needs $m_{12}^2 = m_2^2 - m_1^2 = 10^{-4} - 10^{-11}$ eV² and $m_{23}^2 = m_3^2 - m_2^2 = 10^{-3}$ eV² to account for the solar and atmospheric [11] neutrino problems respectively. The required value of m_{23}^2 is much larger than the value of the effective mass square $2^{-2} G_F E_N e$ of the electron neutrino at the solar core. This suppresses mixing of the third neutrino in matter as well [12] which decouples from the rest in case of the MSW solution to the solar neutrino problem .

Using the mixing matrix (5) the e survival probability in vacuum from Sun to Earth is given by the expressions

$$P_{ee} = c_1^4 + s_1^4 + 2(c_1 s_1)^2 \cos\left(\frac{m_{12}^2 L}{2E}\right) \quad (6)$$

where $L = 1.5 \cdot 10^{13}$ cm = 500.3 s is the Earth-Sun distance.

Using the mixing matrix elements from eq.(5), we find that the expression for $_{eff}^2$ for VO is given by

$$\begin{aligned} (_{eff}^2)_{VO} &= \sum_{ij} U_{ei} e^{iE_i L} \bar{U}_{ej} \\ &= c_1^2 (_{11}^2 + _{12}^2 + _{13}^2) + s_1^2 (_{21}^2 + _{22}^2 + _{23}^2) \\ &\quad + 2c_1 s_1 (_{11} \bar{_{21}} + _{12} \bar{_{22}} + _{13} \bar{_{23}}) \cos\left(\frac{m_{12}^2 L}{2E}\right) \end{aligned} \quad (7)$$

The $_3$ state can be produced after the electron scattering by $_1$ and $_2$ in the solar neutrino beam, therefore the transition moments $_{13}$ and $_{23}$ appear in the expression above. However since the solar neutrino beam does not contain $_3$, there is no $_{3i}$ dependence in $_{eff}^2$ and $_{33}$ cannot be constrained by solar neutrino experiments.

Vacuum solution requires $m_{12}^2 = 10^{-10}$ eV². The oscillatory term in eq.(7) does not get averaged out in this case. This term by itself is not positive definite and prevents obtaining bounds on all the moments appearing in eq.(7). We thus need to make simplifying assumptions. For the case of Dirac neutrinos we assume (as in the Particle Data Book) that the dominant non-zero elements are diagonal $_{ij} = \bar{_{ij}}$. With this assumption, eq.(7) simplifies to the form

$$_{eff}^2 = c_1^2 (_{11}^2 + _{22}^2) + s_1^2 (_{22}^2) : \quad (8)$$

Both these terms are positive definite and we can individually bound each of this term assuming other to be absent. For the case of Majorana neutrinos the magnetic moment matrix $_{ij}$ is anti-symmetric. We set $_{11} = _{22} = 0$ and find that $_{eff}^2$ can be given an upper and lower bounds

$$_{12}^2 + (c_1 j_{13} j_{23} \bar{j})^2 \leq _{eff}^2 \leq _{12}^2 + (c_1 j_{13} j_{23} \bar{j})^2 : \quad (9)$$

From this we see that $_{eff}^2$ can be written as a sum of two positive definite quantities and therefore one can take each term separately in order to put an upper bound on $_{12}^2$. To put bounds on $_{12}^2$ and $_{13}^2$ we need to further assume that there is no cancellation between the two terms in the expression $(c_1 j_{13} j_{23} \bar{j})^2$ ie either $j_{23} \bar{j}$ or $j_{13} \bar{j}$

is much larger than the other.

3. M SW conversion

If the flavor conversion of neutrinos in the Sun is by M SW mechanism then we have different expressions for ν_{eff} . As discussed already, only two energy eigenstates ν_1 and ν_2 corresponding to the lighter neutrinos participate in the M SW conversion. In the core of the Sun $E_1 > E_2$, there is a level crossing at the resonance point after which $E_2 > E_1$ i.e. $m_2 > m_1$ in vacuum. The probability of $\nu_e \rightarrow \nu_1$ just after level crossing is

$$P_1 = P_J s_m^2 + (1 - P_J) c_m^2 \quad (10)$$

Here, the first term stands for ν_e going to ν_2 by mixing with probability s_m^2 and then jumping to ν_1 with probability P_J at the level crossing. The second term means that ν_e goes to ν_1 by mixing and then does not jump to ν_2 with probability $(1 - P_J)$ at the level crossing. The probability of $\nu_e \rightarrow \nu_2$ just after level crossing is

$$P_2 = (1 - P_1) = (1 - P_J) s_m^2 + P_J c_m^2 : \quad (11)$$

In the formulas above, the Landau-Zener jump probability is given by

$$P_J = \frac{\exp(-bs_1^2/E)}{1 - \exp(-b/E)} \quad (12)$$

$$b = \frac{m^2}{4} \frac{A}{A - A_{\text{res}}} \cdot 10^9 \frac{m^2}{eV^2} \text{ M eV} \quad (13)$$

and $A = 2 \frac{P}{2E} G_F N_e$. The mixing angle in matter in the Sun is given in terms of the vacuum mixing angle by the expression

$$\cos 2 \theta_m = \frac{(1 + (1 - 2s_1^2))}{(1 - 2(1 - 2s_1^2) + 2)^{1/2}} \quad (14)$$

$$= \frac{m^2}{A} = 6.6 \cdot 10^{-5} \frac{b}{E} \quad (15)$$

We can now use the matrix eq.(5) to find the survival probability of ν_e at Earth,

$$P_{ee} = c_1^2 P_1 + s_1^2 P_2 \quad (16)$$

Unlike in the vacuum case, $\frac{2E}{m_{12}^2}$ is much smaller than the Sun-Earth distance in case of the M SW conversion. Thus phases acquired in oscillations average out [13]. We can thus drop the interference terms of the type $A_1(L)A_2(L)$ in the expression for ν_{eff} in eq.(3). Substituting for $A_1(L) = P_1$ and $A_2(L) = P_2$ and we then get

$$\begin{aligned} (\nu_{\text{eff}})_M \text{ SW} &= \sum_{ij} \sum_{ij} P_i^2 \\ &= P_1 \frac{2}{11} + \frac{2}{12} + \frac{2}{13} + P_2 \frac{2}{21} + \frac{2}{22} + \frac{2}{23} \\ &= \frac{2}{12} + P_1 \left(\frac{2}{11} + \frac{2}{13} \right) + (1 - P_1) \left(\frac{2}{22} + \frac{2}{23} \right)^2 \end{aligned} \quad (17)$$

Since, $(\nu_{\text{eff}})_M \text{ SW}$ contains a sum of positive definite terms we can put upper bounds on each term taken one at a time, using the expression eq.(10) for P_1 . In this case, we are able to constrain all P_{ij} except P_{33} .

4. Experimental rates and bounds on magnetic moments

The electron scattering reaction in Super-K can be written as

$$R_{SK} = \frac{\int dE_e \int dE_B P_{ee} + \int dE_B \int dE_e (1 - P_{ee}) + \int dE_e \int dE_B m_{\text{ag}}(E) P_{ee}}{\int dE_e \int dE_B} \quad (18)$$

The magnetic moment scattering cross section $m_{\text{ag}}(E)$ is obtained by integrating (w.r.t the electron recoil energy T) the differential cross section σ folded with a detector response function taken from [14]. The ${}^8\text{B}$ flux is taken

from [5] and is given below. Only the Super-K electron elastic scattering rate depends on the neutrino magnetic moments.

The charge-current deuterium dissociation reaction rate at SNO normalized to its SSM value is given by

$$R_{\text{SNO}}^{\text{CC}} = \frac{\int dE \text{CC}_B P_{ee}}{\int dE \text{CC}_B} \quad (19)$$

The ν_e and $\bar{\nu}_e$ elastic scattering cross section after folding with the detector response function are tabulated in ref. [15]. The deuterium dissociation cross section is taken from [16].

The rates of neutrino capture in the Chlorine and Gallium experiments can be written as

$$R = \frac{\int dE \text{X}_i P_{ee}}{\int dE \text{X}_i} \quad (20)$$

where the subscript $i = \text{Ga, Cl}$ denotes the experiment and $i = \text{pp, }^7\text{Be, }^8\text{B}$ denotes the type of neutrino flux from the Sun. The spectra of the pp and ^8B neutrinos can be fitted with the analytical functions,

$$\begin{aligned} \text{pp} &= (5.95 \cdot 10^{10}) [1.93 \cdot 9 (0.931 \cdot E) ((0.931 \cdot E)^2 - 0.261)^{1/2} E^2] \\ \text{B} &= (5.05 \cdot 10^6) [8.52 \cdot 10^6 (15.1 \cdot E)^{2.75} E^2] \\ \text{Be} &= (4.77 \cdot 10^9) [(E - 0.862)] \end{aligned} \quad (21)$$

where the neutrino fluxes are in units of $\text{cm}^{-2} \text{s}^{-1}$ and E is in MeV. The first brackets in (21) give the total flux of neutrinos from the pp, Be, and B reactions and are taken from BP2000 [5], and the square brackets give the spectral shape [17].

The Ga experiments can detect all three types of neutrino fluxes and the neutrino absorption cross section of Ga is given in [18]. The Chlorine experiment threshold is higher (0.8 MeV) and it detects only the Be and B neutrinos; we take the absorption cross section with the tables from ref. [19].

Using the flux spectrum in equation (21) and the cross sections [18,19,15,16] we can calculate the theoretical rates for MSW or VO conversion probabilities as a function of the three unknown parameters: the magnetic moment matrix elements m_{ij} , m_{12}^2 and the vacuum mixing angle θ_1 . The experimental rates R^{expt} with one-sigma combined (statistical and systematic) experimental errors are as follows [14]:

$$\begin{aligned} R_{\text{Cl}}^{\text{expt}} &= 0.335 \pm 0.029 \\ R_{\text{Ga}}^{\text{expt}} &= 0.584 \pm 0.039 \\ R_{\text{SK}}^{\text{expt}} &= 0.459 \pm 0.017 \\ R_{\text{SNO CC}}^{\text{expt}} &= 0.347 \pm 0.029 \end{aligned} \quad (22)$$

From the theoretical R , and the experimental R^{expt} , we compute the total χ^2 for all experiments, defined as

$$\chi^2 = \frac{\sum_i (R_i - R_i^{\text{expt}})^2}{2} \quad (23)$$

Setting the parameter $\text{eff} = 0$ we reproduce the standard contours of VO (Fig. 1.) and MSW (Fig. 2) solutions shown as continuous curves. For $\text{eff} = 0$ the global minimum of χ^2 occurs in the vacuum region with $\text{m}_{12}^2 \approx 0.3$. We then take a non-zero eff and plot the regions (shown as dashed curves) in $\text{m}_{12}^2 - \tan^2 \theta_1$ plane corresponding to $\chi^2_{\text{min}} + 4.6$ (90% CL) both for VO (Fig. 1) and MSW (Fig. 2) solutions. These figures correspond to a constant value for eff . It is found that the allowed regions shrinks as we increase the value of eff and it disappears for some specific eff which is taken to be the 90% CL bound on eff . We consider different cases following this procedure.

In case of VO and Dirac neutrino, we choose eff equal to m_1^2 and m_2^2 (see eq.(8)) respectively. The bounds on m_{12}^2 obtained using the above procedure are given by (at 90% CL):

$$\begin{aligned} \text{m}_1 &< 4.5 \cdot 10^{10} \text{ B} \\ \text{m}_2 &< 7.1 \cdot 10^{10} \text{ B} \end{aligned} \quad (24)$$

In case of the Majorana neutrinos we use eq.(7) and substitute ϵ_{eff}^2 by ϵ_{12}^2 , $\epsilon_1^2 j_{13} j$ or $\epsilon_1^2 j_{23} j$ leading to the 90% CL bounds

$$\begin{aligned} j_{12} j < 3.7 \cdot 10^{10} & \text{ B ;} \\ j_{13} j < 4.5 \cdot 10^{10} & \text{ B (if } j_{23} j < j_{13} \text{)} \\ j_{23} j < 7.1 \cdot 10^{10} & \text{ B (if } j_{13} j < j_{23} \text{)} \end{aligned} \quad (25)$$

Next we take up the M SW solution. We find that the LMA and SMA allowed parameter space disappears for $\epsilon_{\text{eff}} = 3:7$ which translates to the bound on j_{12} . Next we take $\epsilon_{\text{eff}} = (1 - P_1)^2$ and find that the parameter space vanishes when $\epsilon_{\text{eff}} = 4:3$. This translates to the bounds on $j_{22} j_{23} j$. Finally we take $\epsilon_{\text{eff}} = P_1^2$ and find that the SMA region disappears for $\epsilon_{\text{eff}} = 7:8$ and the LMA region disappears at $\epsilon_{\text{eff}} = 20:5$ which translates into the bounds on $j_{11} j_{13} j$. These bounds are summarized below :

$$\begin{aligned} j_{12} j < 3.8 \cdot 10^{10} & \text{ B} \\ j_{22} j_{23} j < 4.3 \cdot 10^{10} & \text{ B} \\ j_{11} j_{13} j < 7.8 \cdot 10^{10} & \text{ B (SMA) ; } 20.5 \cdot 10^{10} \text{ B (LMA)} \end{aligned} \quad (26)$$

In (26), the bounds on the diagonal elements of j_{ij} are relevant for Dirac neutrinos only and the bounds on the off-diagonal elements apply to both Dirac and Majorana neutrinos. The bound on $j_{11} j_{13} j$ obtained in case of the LMA solution is weakest of all bounds. This is due to the fact that these quantities are multiplied by P_1 in eq.(17) which is very small for adiabatic transition occurring in the LMA region.

While the neutrino magnetic moments affect the rates of only the Super-K experiment, a combined analysis of all experiments was essential in establishing the bounds given in eqs.(24-26). This can be seen explicitly in Fig. 3. and Fig. 4 for the VO case and in Fig. 5. and Fig. 6. for the M SW case. In Fig. 3. we plot the 1:64 allowed regions for R_{SK} (continuous line) and R_{SNO} (dotted line) by setting $\epsilon_{\text{eff}} = 0$. We see a large overlap between the SK and SNO allowed regions for $\epsilon_{\text{eff}} = 0$. Next we repeat the same plots by taking $\epsilon_{\text{eff}} = 3:8$. We see that the SK allowed parameter shifts so that there is no more any overlap with the SNO allowed region. Therefore a combination of SNO and SK result is crucial in disallowing $\epsilon_{\text{eff}} > 3:8$.

Similarly in Fig. 5. and Fig. 6. we plot the 1:64 allowed regions for $\epsilon_{\text{eff}} = 0$ and $\epsilon_{\text{eff}} = 4:0$ respectively. In Fig. 5. we see overlap between SK allowed regions (between continuous curves), SNO (between dashed curves) and Gallium (between dotted curves) in the SMA and the LMA regions. In Fig. 6. we see that when $\epsilon_{\text{eff}} = 4:0$ the SK allowed parameter space shifts so that there is no common allowed region for the three experiments thereby ruling out values of $\epsilon_{\text{eff}} > 4:0$.

In summary, we have used solar neutrino rates to constrain possible magnetic moment coupling of neutrinos to photons. The bounds depend upon specific solution of the solar neutrino problem. If M SW mechanism is mainly responsible for the solar neutrino conversion then it is possible to constrain all elements of magnetic moment operator j_{ij} except for j_{33} . For the VO solution one can obtain bounds (eq.(24)) on two of the diagonal elements assuming a diagonal j_{ij} in case of the Dirac neutrinos. For Majorana neutrinos, we obtain bounds on j_{12} , j_{13} and j_{23} given in eq.(25).

[1] B. T. Cleveland et al, *Astrophys. J.* 496, 505 (1998).
[2] J. N. Abdurashitov et al. [The SAGE collaboration], *Phys. Rev. C* 60, 055801 (1999);
W. Hambrecht et al. [The Gallex collaboration], *Phys. Lett. B* 447, 127 (1999);
M. A. Immann et al. [The GNO collaboration], *Phys. Lett. B* 492, 16 (2000).
[3] Y. Fukuda et al [The Super-Kamiokande collaboration], *Phys. Rev. Lett.* 86, 5651 (2001);
Y. Fukuda et al *Phys. Rev. Lett.* 85, 3999 (2001).
[4] Q. R. Ahmad et al. [SNO Collaboration], *Phys. Rev. Lett.* 87, 071301 (2001).
[5] J. N. Bahcall, M. H. Pinsonneault and S. Basu, *Astrophys. J.* 555, 990 (2001).
[6] S. N. Gninenko, *Phys. Lett. B* 452, 414 (1999); *Mod. Phys. Lett. A* 13 1791, (1998); *Phys. Lett. B* 427 206 (1998);
S. Gninenko and N. V. Krasnikov, *Phys. Lett. B* 490 9 (2000).
[7] J. F. Beacom and P. Vogel, *Phys. Rev. Lett.* 83, 5222 (1999).
[8] A. Joshipura and S. Mohanty, Bounds on neutrino magnetic moments and charge radii from Super-K and SNO observations, *Archive hep-ph/0108018*.

[9] S. Choubey, S. Goswami, and D. Majumdar, Phys. Lett. B 484, 73 (2000); Phys. Rev. D 63, 113019 (2001); hep-ph/0204173;
 A.S. Joshipura, E. Masso and S. Mohanty, hep-ph/0203181;
 J.F. Beacom and N.F. Bell, hep-ph/0204111.

[10] M. Apollonio et al., Phys. Lett. B 466, 415 (1999).

[11] Y. Fukuda et al. [The Super-Kamiokande collaboration], Phys. Rev. Lett. 81, 1562 (1998).

[12] A.S. Joshipura and P. Krastev, Phys. Rev. D 50, 3484 (1994).

[13] A.S. Dighe, Q.Y. Liu and A.Yu. Smirnov, hep-ph/9903329.

[14] G.L. Fogli, E. Lisi, A. Palazzo, F.L. Villante, Phys. Rev. D 63, 113016 (2001).

[15] J. Bahcall, P. Krastev, and E. Lisi, Phys. Rev. C 55, 494 (1997).

[16] J. Bahcall and E. Lisi, Phys. Rev. D 54, 5417 (1996).

[17] J.N. Bahcall and R.K. Ulrich, Rev. Mod. Phys. 60, 297 (1988);
 J.N. Bahcall and B.R. Holstein, Phys. Rev. C 33, 2121 (1986).

[18] J.N. Bahcall, Phys. Rev. C 56, 3391 (1997).

[19] J. Bahcall et al., Phys. Rev. C 54, 411 (1996).

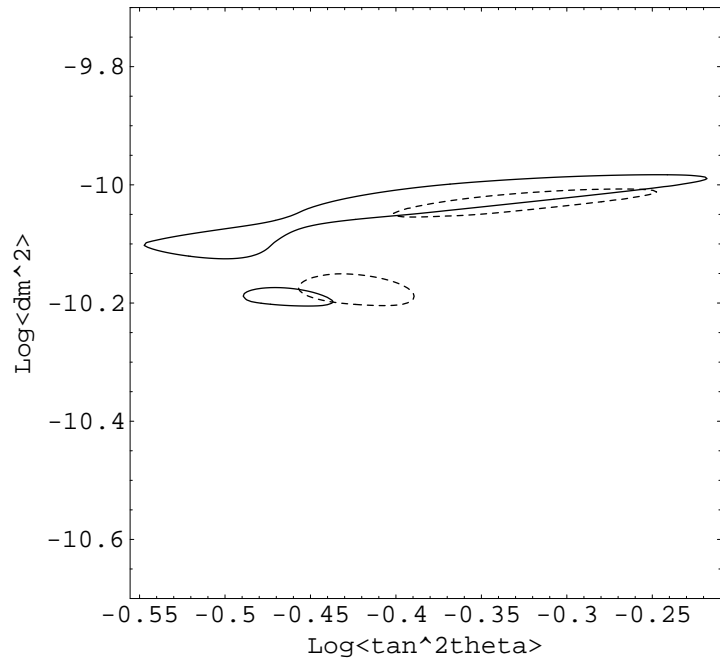


FIG.1. The 90% allowed parameter space for VO , with $_{eff} = 0$ (enclosed by continuous curve) and for $_{eff} = 3$ (enclosed by dashed curve).

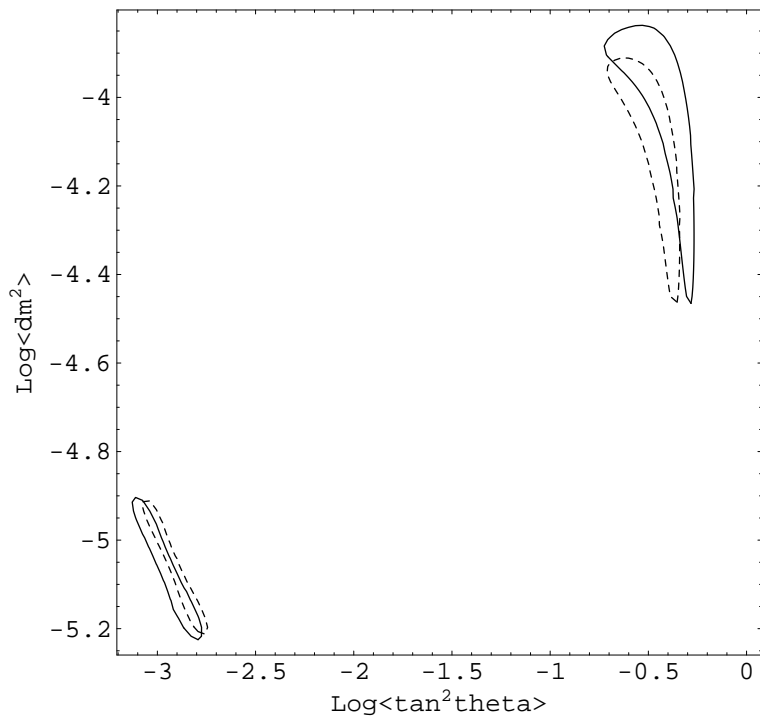


FIG.2. The 90% allowed parameter space for VO , with $_{eff} = 0$ (enclosed by continuous curve) and for $_{eff} = 3$ (enclosed by dashed curve).

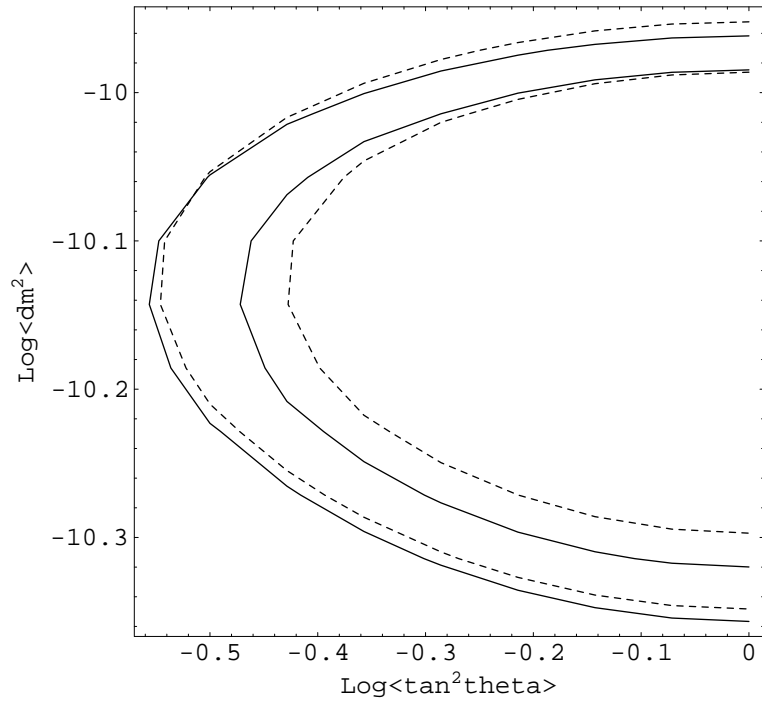


FIG .3. The 1:64 VO allowed regions for R_{SN0} (enclosed by dashed curves) and R_{SN0}^* (enclosed by continuous curves) for $_{eff} = 0$.

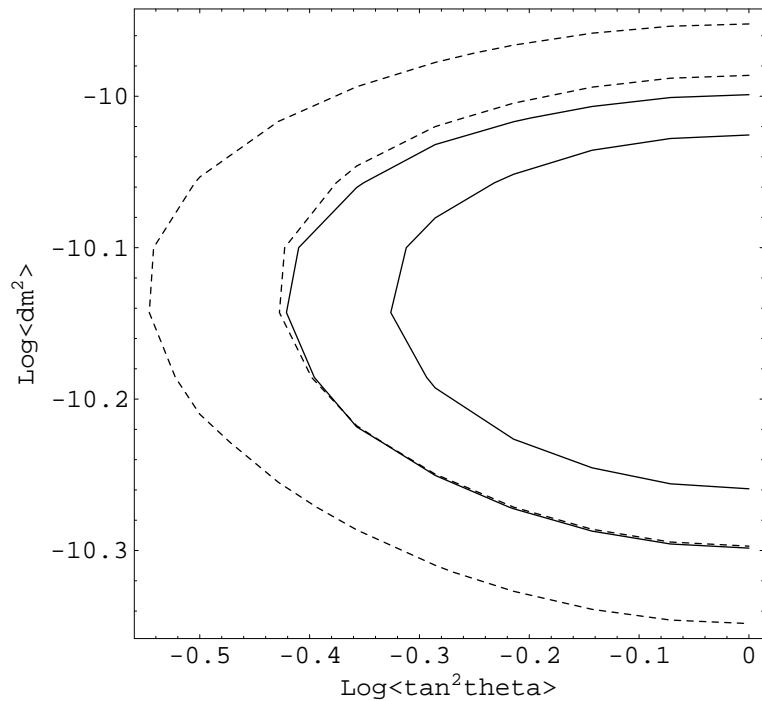


FIG .4. The 1:64 VO allowed regions for R_{SN0} (enclosed by dashed curves) and R_{SN0}^* (enclosed by continuous curves) for $_{eff} = 3.8$.

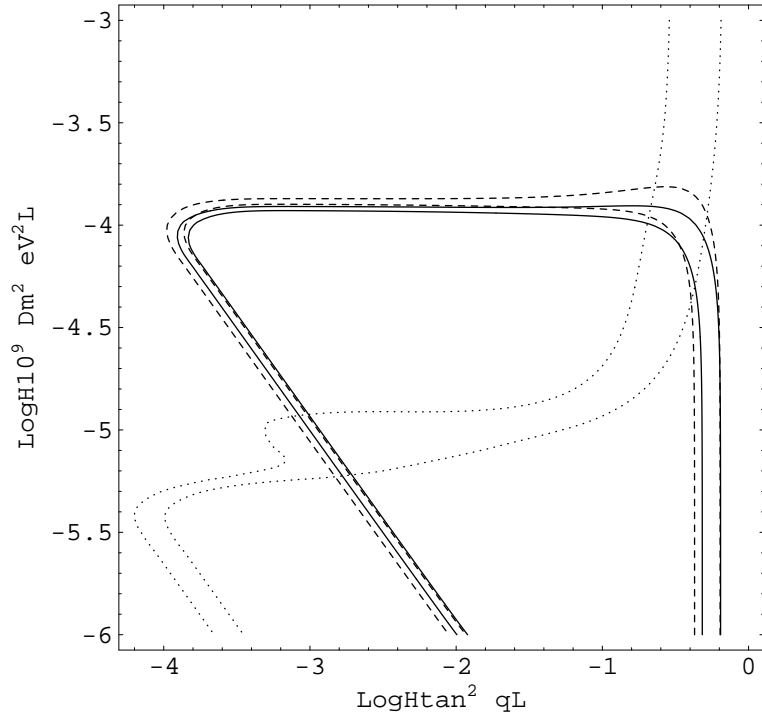


FIG. 5. The 1:64 MSW allowed regions for R_{SNO} (enclosed by dashed curves) and R_{SNO} (enclosed by continuous curves) and R_{Ga} (enclosed between dotted curves) for $\epsilon_{eff} = 0$. There is overlap in the SM A and LM A regions.

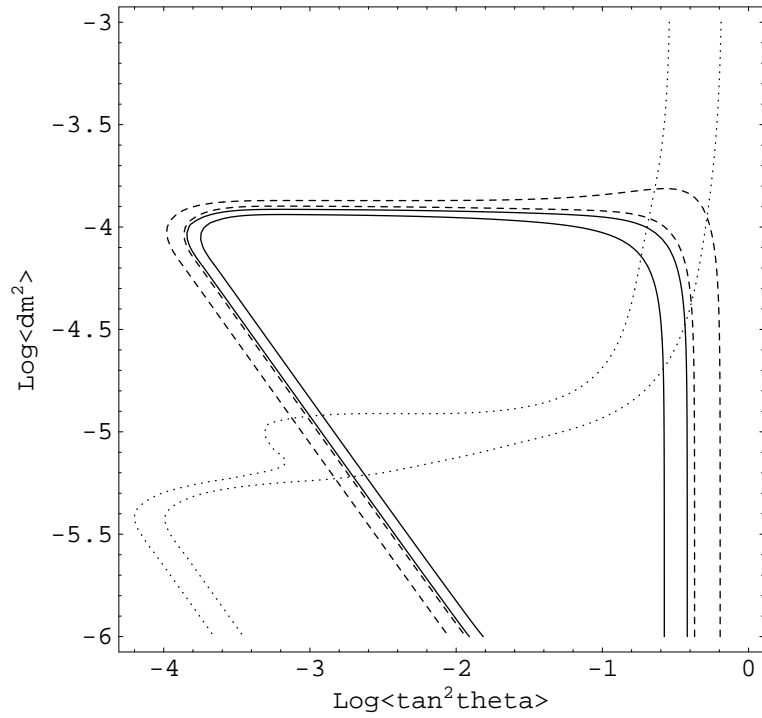


FIG. 6. The 1:64 MSW allowed regions for R_{SNO} (enclosed by dashed curves) and R_{SNO} (enclosed by continuous curves) and R_{Ga} (enclosed between dotted curves) for $\epsilon_{eff} = 4$. The SK allowed region shifts such that there is no overlap between the three.